THE JOURNAL OF PHYSICAL CHEMISTRY C

Article

pubs.acs.org/JPCC

Stability and Surface Reconstruction of Topological Insulator Bi_2Se_3 on Exposure to Atmosphere

Mark T. Edmonds,[†] Jack T. Hellerstedt,[†,‡] Anton Tadich,[§] Alex Schenk,[∥] Kane Michael O'Donnell,[§,⊥] Jacob Tosado,[†,‡] Nicholas P. Butch,[‡,#] Paul Syers,[‡] Johnpierre Paglione,[‡] and Michael S. Fuhrer*[,†,‡]

[†]School of Physics, Monash University, Clayton, VIC 3800, Australia

[‡]Center for Nanophysics and Advanced Materials, University of Maryland, College Park, Maryland 20742-4111, United States

[§]Australian Synchrotron, 800 Blackburn Road, Clayton, VIC 3168, Australia

[∥]Department of Physics, La Trobe University, Bundoora, VIC 3086, Australia

[⊥]Department of Imaging and Applied Physics, Curtin University, Bentley, WA 6102, Australia

[#]National Institute of Standards and Technology, Gaithersburg, Maryland 20899, United States

ABSTRACT: The stability of the surface of vacuum-cleaved topological insulator Bi_2Se_3 single crystals is investigated with high-resolution synchrotron-based photoelectron spectroscopy. While the surface is stable at room temperature in vacuum, a Bi_2 layer always forms at the surface of Bi_2Se_3 upon even brief (5 min) exposure to atmosphere. This is accompanied by a depletion of selenium in the near surface region and a 1.4 eV decrease in work function. The Bi_2 surface is found to be stable upon return to ultrahigh vacuum conditions but is unstable with prolonged exposure to air, ultimately resulting in two possible different reconstructed surfaces, explaining previous contradictory results on long-term atmosphere exposure of Bi_2Se_3.

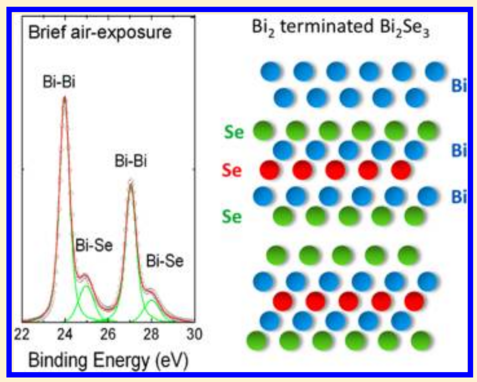

■ INTRODUCTION

Topological insulators, such as Bi_2Se_3, are a new class of material that possess topologically protected helical metallic surface states and a bulk band gap. These three-dimensional topological insulators hold great promise for future nanoelectronic devices including spin generation and detection without ferromagnetism, dissipationless electronic transport in the quantum anomalous Hall state,[1−3] and the ability to host exotic bound edge states when interfaced with other materials.[4] However, unanswered questions remain regarding the fate of the Bi_2Se_3 surface upon exposure to the atmosphere. Importantly, while the topology of Bi_2Se_3 guarantees the presence of a metallic surface, the topological properties of the metallic surface, including the presence of nontopological bands overlapping in energy, depend on the details of the surface and its reconstruction.[5,6] Thus, it is essential to understand the structure of the air-exposed Bi_2Se_3 surface in order to interpret the properties of any air-exposed Bi_2Se_3 device.

Given the rhombohedral crystal structure of Bi_2Se_3, with weak van der Waals bonding between adjacent selenium planes joining Se−Bi−Se−Bi−Se quintuple layer units, it is expected that the surface would be selenium-terminated postcleaving.[7,8] However, a recent study using low-energy ion scattering and density functional theory (DFT) suggests that bismuth termination is the most energetically favored, and a transition from selenium to bismuth termination takes place postcleaving,[9] although another study using low-energy electron diffraction and surface X-ray scattering found the expected selenium termination.[10] Furthermore, significant debate exists in the literature on the effect of air exposure to vacuum-cleaved Bi_2Se_3 single crystals, with conflicting reports of rapid oxidation after 2 days air exposure[11] and negligible surface reactivity after months of exposure.[12,13] A recent study found two different surface terminations for samples cleaved in air, but only selenium terminations for vacuum-cleaved crystals.[7] A careful study on the evolution and fate of the surface of vacuum-cleaved Bi_2Se_3 on exposure to atmosphere is needed to reconcile the diverse and contradictory observations in the literature. Most notably, no study has examined the immediate effects of air exposure on the vacuum-cleaved surface, with previous studies typically investigating exposure times of days[11,12] or samples cleaved *ex situ*.[7]

Here we report high-resolution photoemission spectroscopy of lightly doped Bi_2Se_3 crystals (surface Fermi energy relative to Dirac point $E_F - E_D \sim 270$ meV) cleaved in a vacuum. We find that the vacuum-cleaved surface is invariably selenium terminated and is stable in vacuum for at least 1 week. We then studied the changes to the vacuum-cleaved surface with brief exposure to atmosphere (5 min) before reintroduction into vacuum and longer air exposure (days). Surface-sensitive

Received: June 18, 2014
Revised: August 5, 2014
Published: August 21, 2014

dx.doi.org/10.1021/jp506089b | *J. Phys. Chem. C* 2014, 118, 20413−20419

photoemission spectroscopy (photon energy $h\nu$ = 100 eV) of the Bi 5d and Se 3d core levels allows accurate surface-sensitive observation of the evolution of composition of the Bi_2Se_3 surface upon air exposure, while low-energy secondary electron cutoff spectroscopy allowed measurement of change to the work function. Upon brief atmospheric exposure we consistently observe (in 7 out of 7 samples) the formation of an elemental bismuth layer at the surface of Bi_2Se_3, coinciding with a depletion of selenium from the uppermost surface layers and a reduction in work function of 1.4 eV. These findings demonstrate that Bi_2Se_3 single crystals exposed to atmosphere undergo an immediate reconstruction at the surface to form a Bi_2 layer that is ~0.8 nm thick. Prolonged air exposure is shown to have markedly different effects on two identically prepared crystals from the same growth; in one case we observe the formation of bismuth oxide consistent with oxidation of the elemental bismuth surface layer, while another sample returned to a state consistent with Bi_2Se_3 termination with little oxidation. These two different ultimate surface terminations, both occurring through the intermediate phase of the Bi terminated surface, explain the previous apparently contradictory results in the literature.[7,11−13]

EXPERIMENTAL METHODS

Low-doped (carrier density ~10^{17} cm^{-3}) bulk Bi_2Se_3 single crystals with bulk resistivity exceeding 2 mΩ cm^{-1} at 300 K were grown by melting high purity bismuth (6 N) and selenium (5 N) in sealed quartz ampules.[14] Crystals used in this experiment were all taken from the same growth and then mounted to a sample holder using conductive epoxy, with a cleaving post subsequently attached to the crystal surface. The samples were then introduced into the ultrahigh vacuum photoemission endstation at the soft X-ray beamline, Australian Synchrotron, where they were subsequently cleaved *in situ*, and then photoelectron spectroscopy measurements were performed immediately at $P \sim 10^{-10}$ mbar. The size of the illuminated area is approximately 100 μm × 20 μm; multiple spots on each sample under investigation were measured postcleaving and after air exposure. The peak intensity of the Bi and Se core levels and all components within (i.e., Bi−Bi and Bi−Se) were found to be uniform across the sample. Zoom lens cameras and the sample manipulator were used to track measurement positions, with a consistent measurement position used throughout the course of measurements on each sample. Samples were exposed to atmosphere via venting the lock load with nitrogen gas and then exposing the sample to ambient conditions for 5 min. Both the Bi 5d and Se 3d core level components of Bi_2Se_3 were measured at a photon energy of 100 eV to ensure high surface sensitivity with an overall measurement uncertainty of ±0.02 meV. The work function was determined from the secondary electron cutoff spectra with an experimental uncertainty of ±0.03 meV. The binding energy scales of all Bi_2Se_3 related spectra are referenced to the Fermi energy (E_F), determined either using the Fermi edge or setting the binding energy of the Au $4f_{7/2}$ core level to be 84.00 eV for an Au reference in electrical contact with the sample. Core level spectra were analyzed using a Shirley background subtraction and then peak fitted using Voigt functions for each peak component, where the Gaussian and Lorentzian widths of the Bi 5d and Se 3d core level parameters were taken from ref 15. Error bars associated with measurements and fits correspond to one standard deviation unless otherwise noted.

RESULTS

The effect of air exposure to Bi_2Se_3 proceeds in two parts, which are (i) immediate effect of air exposure and (ii) prolonged air exposure.

Immediate Effect of Air Exposure on Bi_2Se_3. Figure 1 shows photoelectron spectroscopy measurements of the Bi 5d and Se 3d core levels and also the low-energy cutoff spectra measured after *in situ* vacuum cleaving and upon reintroduction to UHV after a 5 min air exposure of the Bi_2Se_3 (sample S1). In Figure 1a, the Bi 5d core level is shown in the upper panel after vacuum cleaving without exposure to air; the lower panel shows the Bi 5d core level of the same sample after air exposure. After cleaving, the core level contains only the characteristic doublet representing the Bi $5d_{5/2}$ and Bi $5d_{3/2}$ orbitals with peak positions of 24.86 and 27.89 eV, respectively. We label these peaks Bi−Se, and as discussed in further detail below, we identify them as characteristic of bismuth bonded to selenium within the Bi_2Se_3 quintuple-layer unit. These peak positions are consistent with previous measurements on these low-doped crystals[16] and other Bi_2Se_3 crystals.[12] After the 5 min air exposure a new component appears at 1 eV to the lower binding energy side of the Bi−Se doublet, labeled Bi−Bi at 23.86 and 26.89 eV, respectively, consistent with elemental bismuth.[17] The Bi−Bi component has a peak area 4 times larger than the Bi−Se component, which now appears as a small shoulder in the spectra. The Bi−Se component has also shifted 0.1 eV to higher binding energy from the as-cleaved position, indicative of the Fermi level moving 0.1 eV further away from the Dirac point. This signifies population of the bulk conduction band and large increase in n-type doping, which is consistent with previous reports of increased electron doping after exposure to water vapor or aging in vacuum.[18,19]

To examine this additional Bi−Bi component, measurements were performed at photon energies between 100 and 850 eV (as shown in Figure 1b) in order to increase the photoelectron mean free path (or probing depth). In Figure 1b as the photon energy increases (i.e., the emitted photoelectrons possess a larger kinetic energy) the Bi−Se peak increases, while the Bi−Bi peak decreases. This demonstrates that the additional Bi−Bi peak relates solely to the near surface of the crystal and not the bulk. A small shoulder to higher binding energy of the Bi $5d_{5/2}$ and Bi $5d_{3/2}$ orbitals is also identified, indicating a small amount of oxidation.

Turning to the Se 3d core level, we plot the as-cleaved (black squares) and air-exposed (red circles) spectra in Figure 1c. Unlike the Bi 5d core level for both as-cleaved and air-exposed, the Se 3d core level contains only a single doublet representing the Se $3d_{5/2}$ and Se $3d_{3/2}$ orbitals. After air exposure a large reduction in intensity is observed, with the peak area of the core level after air exposure 4 times smaller than as-cleaved. This reduction is quantitatively consistent with the 4:1 ratio of the Bi−Bi to Bi−Se peak intensity observed in the lower panel of Figure 1a, strongly suggesting that selenium is associated only with Bi_2Se_3 units responsible for the Bi−Se peak and no selenium is associated with the Bi−Bi peak. Furthermore, the peak position of both orbitals shift to higher binding energy by ~0.45 eV after air exposure, which is 0.35 eV more than observed for the Bi 5d core level. Finally, we examine in Figure 1d the change in the low-energy cutoff spectra for as-cleaved (black) and air-exposed (red) Bi_2Se_3. The work function of the as-cleaved Bi_2Se_3 is measured to be 5.4 eV, consistent with previous reports.[16] Upon exposure to atmosphere the work

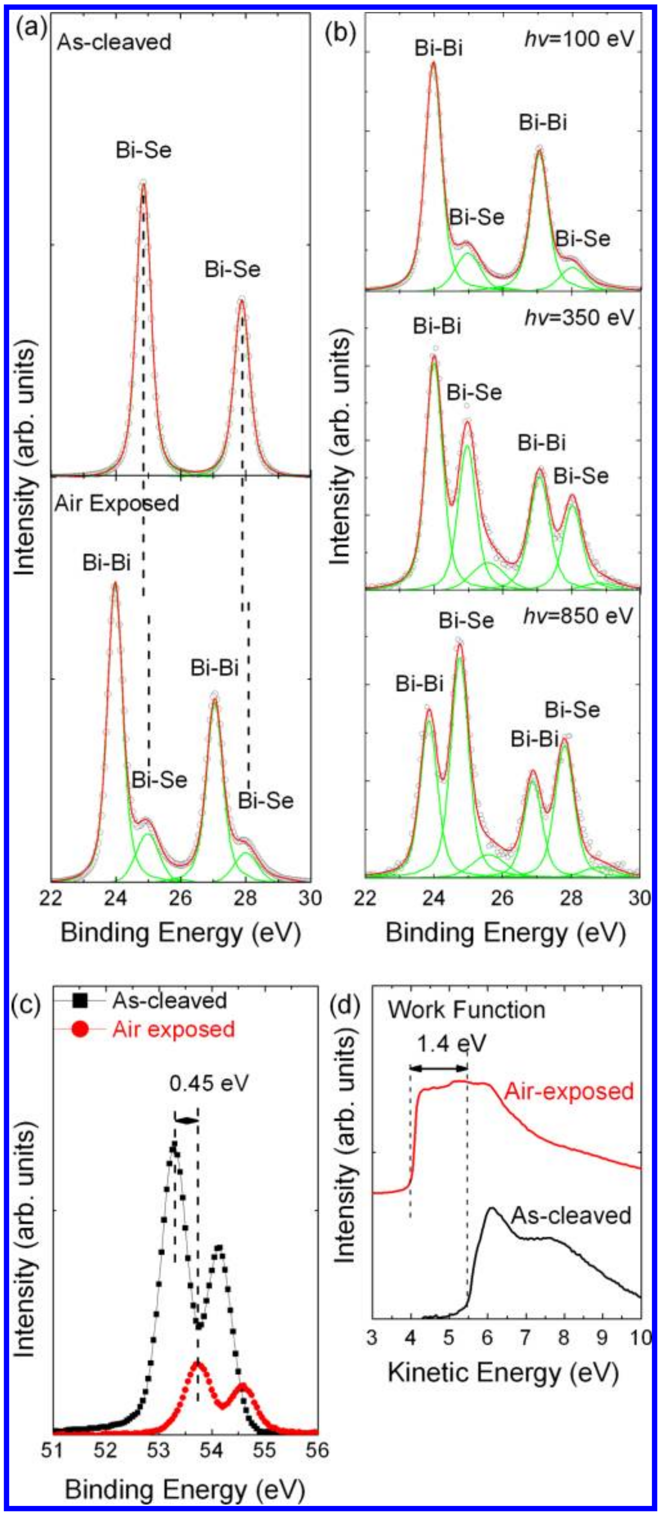

Figure 1. Core level measurements on Bi_2Se_3 crystals after cleaving and postexposure to atmosphere on sample S1. (a) Bi 5d core level taken at 100 eV where the upper panel represents the as-cleaved surface and the lower panel represents the air-exposed surface. (b) Photon energy dependent measurements of the Bi 5d core level taken at 100, 350, and 850 eV for the upper, middle, and lower panels, respectively. (c) Se 3d core level taken at 100 eV for the as-cleaved (black) and air-exposed (red) surfaces. (d) Secondary electron cutoff spectra measured for as-cleaved (black) and air-exposed (red) Bi_2Se_3.

function decreases to 4.0 eV, a difference of 1.4 eV from the as-cleaved state. The sample was then left under UHV conditions for 3 days but showed negligible change to the Bi 5d and Se 3d core levels.

The positions of the Bi−Bi components in Figure 1a are very similar to that reported for Bi_2-terminated surface regions of Bi_4Se_3, which consists of single Bi_2 layers interleaved with single Bi_2Se_3 layers.[5] The agreement between peak positions and the accumulation of bismuth and depletion of selenium in the near surface regime suggests that layers of Bi_2 are spontaneously forming at the surface of Bi_2Se_3 upon exposure to atmosphere. This is further confirmed from the reduction in work function to 4.0 eV after air exposure, which is similar to the work function of Bi(111) of 4.2 eV.[20] The 0.2 eV difference is reasonable given that we are dealing with few-layer isolated Bi_2. The height of single Bi_2 and Bi_2Se_3 layers is known to be 0.4 and 0.8 nm, respectively, from scanning tunneling microscopy.[5] From Figure 1 we assume after air exposure that a layered structure forms with the Bi_2 layers on top and the Bi_2Se_3 underneath. From the ratio of peak areas of the Bi−Se and Bi−Bi components the thickness of the Bi_2 can be determined using the relation $d = \lambda \ln(I_{Bi-Bi}/I_{Bi-Se} + 1)$, where λ is the photoelectron mean free path.[21] From the 100, 350, and 850 eV spectra in Figure 1b we determine an average value for the thickness of the Bi_2 of 0.7 ± 0.1 nm. This is almost twice the thickness of a single Bi_2 layer, suggesting that two layers of Bi_2 form at the surface of Bi_2Se_3 upon air exposure. The consistent observation of a Bi 5d doublet only slightly shifted from that of pristine Bi_2Se_3, and only a single Se 3d doublet after air exposure, indicates that the Bi_2Se_3 unit below the Bi_2 layer is largely unmodified. However, a small but consistent difference in chemical shifts (~0.35 eV; see also data for additional samples below) for Bi and Se may indicate a weak chemical effect of the Bi_2 layer(s) on the underlying Bi_2Se_3.

We now turn to the origin of the Bi−Bi peak and the depletion of selenium in the near surface regime as a result of air exposure. The key to this reconstruction at the surface is exposure to atmosphere, as vacuum-cleaved samples subsequently left in vacuum for several days are not observed to form this Bi_2 layer. In ref 7 it was observed that some air-cleaved Bi_2Se_3 crystals had Bi-rich surface terminations. The authors of that work concluded that the surface termination was the result of intercalation of the crystals with ambient species which produced a greater likelihood of cleaving between the Bi and Se planes of the Bi_2Se_3 unit. However, we can eliminate this mechanism as it does not explain how the Bi_2Se_3 termination in vacuum is transformed to a Bi-rich termination after air exposure. Instead, our results indicate the accumulation of Bi or depletion of Se at the surface may arise as a result of two possibilities. The first is that selenium is volatile with a high vapor pressure and is also known to react with water; thus, the observed reduction in selenium near the surface may be the result of selenium desorption in the form of gas-phase dimers or hydrogen selenide gas.[22] While we cannot rule out this possibility, we find it unlikely, since we observe the Bi_2Se_3 surface to be stable in a vacuum, suggesting selenium desorption is negligible, and ~10 nm capping layers of selenium are regularly used for transporting Bi_2Se_3 samples between UHV chambers for experiments, calling into question the reactivity of selenium upon exposure to atmosphere. The second possibility is that the accumulation of additional bismuth at the surface is a result of diffusion from the bulk. In thin film growth bismuth is known as a surfactant due to its low solid solubility and has a propensity to collect at surfaces in stable configurations despite lattice mismatch and strain to reduce overall surface energy.[23−25] Indeed, first-principles calculations indicate the favorable energetics of the Bi_2 layer atop Bi_2Se_3.[9] Selenium vacancies are inevitable in Bi_2Se_3 and exist in concentrations $>10^{17}$ cm^{-3} even in our low-doped crystals. We hypothesize that the nucleation of the energetically stable bismuth bilayer region at the surface through e.g. desorption of a small amount of selenium could seed the segregation of mobile bismuth or bulk selenium vacancies at the surface, allowing the bismuth bilayer to grow rapidly.

Longer Term Effect of Air Exposure to Bi_2Se_3. With the rapid reconstruction of the Bi_2Se_3 surface upon brief air exposure now revealed we turn to the fate of the surface upon longer term exposure of Bi_2Se_3 in air. This is achieved by performing a series of measurements on two Bi_2Se_3 crystals taken from the same growth (denoted S2 and S3) mounted on a single sample holder directly after cleaving, and after 5 min, 1 day, and 3 day exposures to atmosphere. The results are shown in Figures 2 and 3 where (a) represents S2 and (b) S3 (multiple positions were measured on each sample to ensure uniform behavior). The figures depict the evolution of the Bi 5d and Se 3d core levels with air exposure, respectively, where the upper panel, middle, and lower panels are 5 min, 1 day, and 3 day air exposures. We have omitted the as-cleaved spectra as they are identical to the spectra in Figure 1a,c.

Beginning with the Bi 5d core level in Figure 2, the upper panel clearly shows that the Bi 5d core level of both S2 and S3 closely resembles the core level spectra of S1 in the lower panel of Figure 1a. This demonstrates that the Bi_2 layer reliably forms across multiple samples after 5 min air exposure, all with a similar ratio of the Bi−Bi and Bi−Se components and an almost negligible Bi−O peak. It is after 1 day exposure that a drastic difference appears between the two samples. For S2 a large Bi−O component has developed at 25.84 and 28.86 eV as a result of oxidation,[17] with a small shoulder to lower binding energy representing the Bi−Se component. As shown in Figure 2c, the Bi−Se component saturates at 0.17 eV higher in binding energy than the as-cleaved position, representing increased n-type doping with the Fermi level now residing deep into the bulk conduction band. The Bi−Bi component is noticeably absent for S2 after 1 day of exposure, suggesting that the Bi_2 layers have become completely oxidized upon continued exposure to atmosphere. Turning to the behavior of S3 over time, it is completely different to that of S2 and has returned to the characteristic doublet representing the 5/2 and 3/2 orbitals of bulk Bi_2Se_3 as depicted in Figure 1a, albeit with a shift of +0.08 eV from the as-cleaved position indicating n-type doping. However, most importantly there are no Bi−Bi and Bi−O components visible in the spectra. This demonstrates that not only does the surface of S3 not oxidize with continued air exposure but that selenium has returned to the near surface region in the ordered atomic planes customary to Bi_2Se_3. This is indeed confirmed in Figure 4 where we compare the peak intensity of the Se 3d core level of S3 postcleaving (black), after 5 min (red), and 1 day (blue) air exposure. The clear decrease in intensity upon 5 min air exposure consistent with selenium depletion is observed, followed by the large increase in intensity after 1 day of air exposure to almost the same value obtained directly after cleaving.

With such a marked difference in the Bi 5d core level of S2 and S3, we turn to the Se 3d core level of S2 and S3 in Figure 3 to determine the cause of this difference in sample behavior with prolonged air exposure. After 5 min air exposure the only difference between the samples is that S3 contains a small doublet to higher binding energy that represents a small amount of neutral selenium. At 1 day air exposure there is a large difference in the spectra. The S2 spectra contain three distinct doublets: The doublet at the lowest binding energy

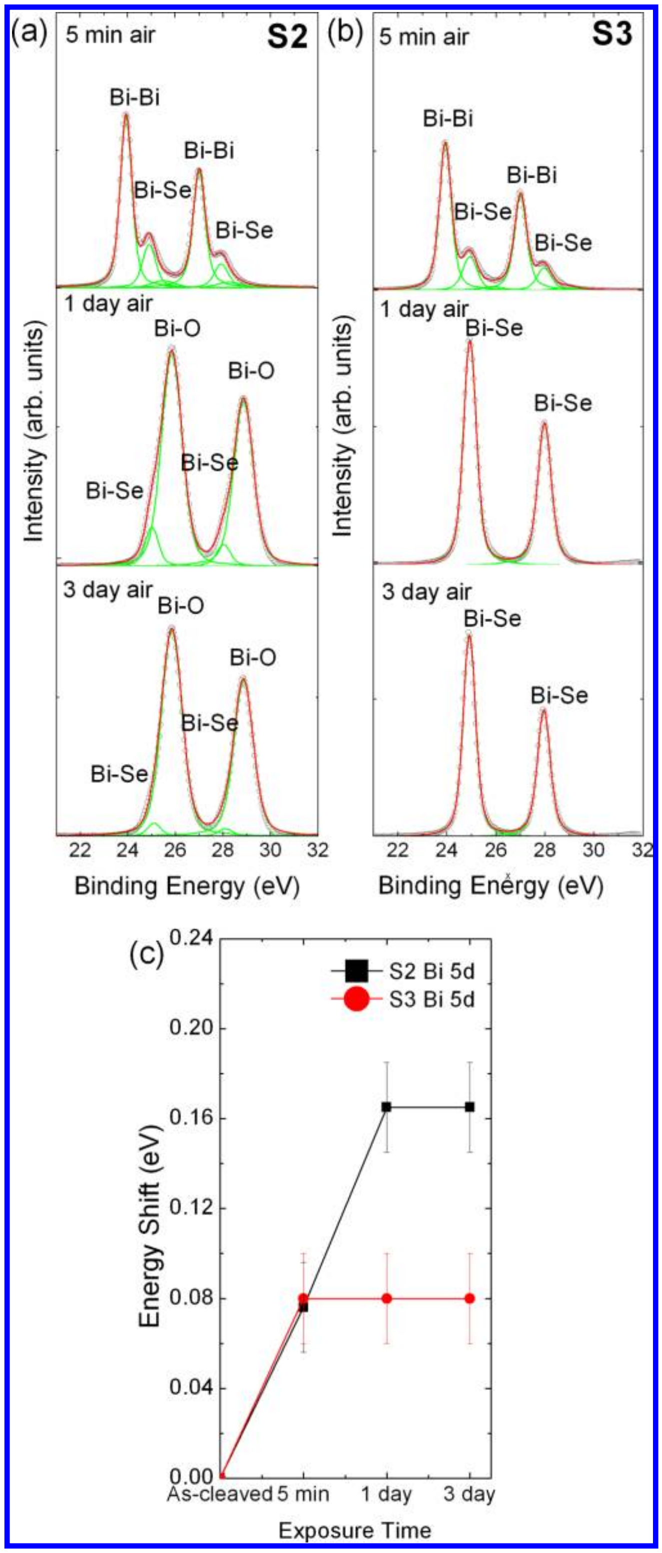

Figure 2. Bi 5d core level measurements after air exposure on Bi_2Se_3 samples: (a) S2 and (b) S3. Upper, middle, and lower panels represent exposure to atmosphere for 5 min, 1 day, and 3 days, respectively. (c) Energy shift of the Bi−Se component as a function of exposure time for S2 (black squares) and S3 (red circles).

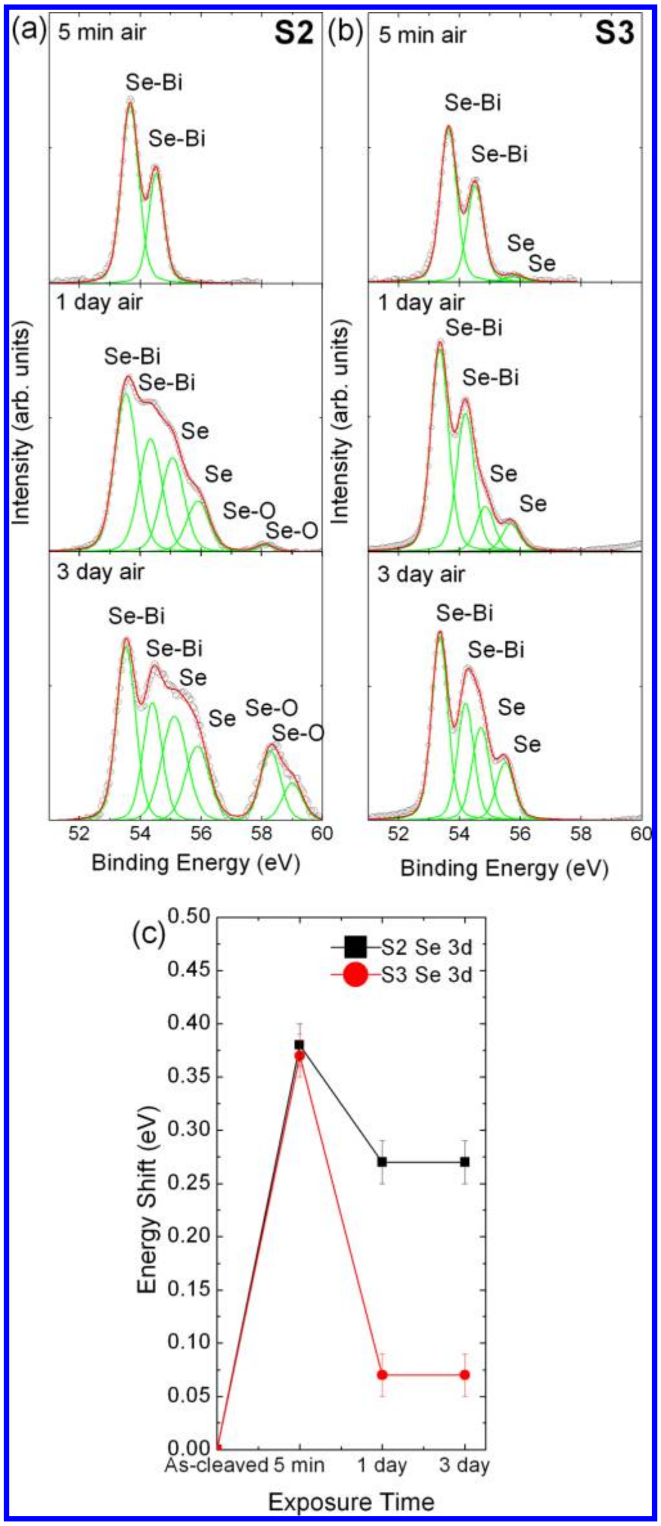

Figure 3. Se 3d core level measurements after air exposure on Bi_2Se_3 samples: (a) S2 and (b) S3. Upper, middle, and lower panels represent exposure to atmosphere for 5 min, 1 day, and 3 days, respectively. (c) Energy shift of the Se−Bi component as a function of exposure time for S2 (black squares) and S3 (red circles).

represents the Bi_2Se_3 peak, shifted +0.27 eV from the as-cleaved position (as depicted in Figure 3c). This is followed by a doublet representing neutral selenium at 55.06 and 55.91 eV, and then a small oxide doublet above 58 eV in binding energy.[17] Further air exposure (as seen in the lower panel) sees

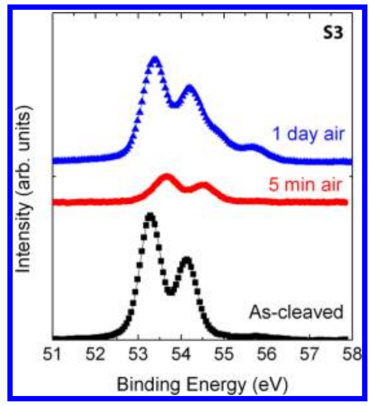

Figure 4. Se 3d core level spectra taken on Bi_2Se_3 sample S3 for the as-cleaved surface (black), after 5 min air exposure (red), and after 1 day air exposure (blue). The additional peaks at 1 day correspond to neutral selenium.

an increase in the neutral selenium and a significant increase in the oxide, with the Se−Bi peak binding energy remaining constant. In comparison, S3 contains no oxide peak and only a slight increase in the neutral selenium doublet. As mentioned earlier, the peak intensity of the Se−Bi component returns to almost the same level of the as-cleaved state. The selenium doublet representing neutral selenium is ∼0.2 eV lower in binding energy at 54.86 and 55.71 eV than S2. This is expected given the difference in binding energy of 0.2 eV between S2 and S3 of the Se−Bi component after 1 day air exposure as shown in Figure 3c. Further air exposure causes a further increase in the amount of neutral selenium but no change in binding energy.

Our observations naturally explain the apparent contradiction in the literature regarding the long-term air stability of the Bi_2Se_3 surface. Sample S2 is clearly oxidized, consistent with the observations in ref 11. Sample S3 appears similar to vacuum-cleaved Bi_2Se_3 even after long-term air exposure; notably it shows no sign of Bi−O or Se−O bonding. This is similar to the observations of refs 12 and 13. However, in our case we are certain that sample S3 has undergone significant reconstruction to a Bi-rich termination immediately after air exposure, followed by additional reconstruction to its final state which appears to be Bi_2Se_3 terminated. The final sample shows notable differences from the vacuum-cleaved sample: it has higher n-doping and a measurable concentration of neutral selenium near the surface. Of course, it is also no longer susceptible to the formation of the Bi-rich termination as observed for vacuum-cleaved samples on air exposure. The microscopic structure of this sample type, and the mechanism of the second reconstruction, will require further study, and the uncontrolled differences which differentiate the two sample types will need to be elucidated. We note that the two samples studied here are nominally identical (i.e., taken from the same growth); however, we cannot be certain that there are no significant differences in e.g. selenium vacancy concentrations that could drive the different reconstruction pathways.

■ CONCLUSION

In conclusion, we reveal that air exposure for time periods as short as 5 min causes a drastic change to the surface of Bi_2Se_3. Utilizing high-resolution surface sensitive photoelectron spectroscopy measurements, we observe an additional component within the Bi 5d core level after air exposure that corresponds to the formation of isolated Bi_2 layers at the surface of Bi_2Se_3. This coincides with a large reduction in intensity from the Se 3d core level, consistent with depletion of selenium in the near surface region. The formation of a Bi_2 layer is found to occur across multiple samples and is precipitated rapidly by exposure of samples to atmosphere, while samples left for several days in UHV after *in situ* cleaving show no change. The Bi_2 surface is found to be stable upon return to ultrahigh-vacuum conditions but is unstable with prolonged exposure to air. Prolonged air exposure produces one of two reconstruction pathways: in the first the Bi_2 layer oxidizes completely, and in the second the surface returns to a state which is similar to the vacuum-cleaved Bi_2Se_3 but with greater n-doping and a notable presence of neutral selenium.

The results have significant consequences for understanding the electronic structure of the air-exposed Bi_2Se_3 surface and call into question the assumption that the surface can be treated as terminated by the Bi_2Se_3 quintuple-layer unit. In contrast to the single topological surface state band at the surface of Bi_2Se_3, Bi-terminated Bi_4Se_3[5] and bismuth bilayers grown on Bi_2Te_3[26] have been shown theoretically and experimentally to have multiple surface bands existing at the Fermi energy and if the bismuth layers are incomplete could also presumably exhibit unusual 1D states at the bismuth adlayer edges. The observation of a stable Bi_2 layer on the Bi_2Se_3 surface at room temperature also offers new possibilities to study a 2D topological insulator (Bi_2) interfaced with a 3D topological insulator (Bi_2Se_3) and suggests new routes to the isolation of 2D Bi_2 on other van der Waals surfaces in order to realize a system in the quantum spin Hall state.[27]

■ AUTHOR INFORMATION

Corresponding Author

*E-mail michael.fuhrer@monash.edu; Tel +61 3 9905 1353 (M.S.F.).

Notes

The authors declare no competing financial interest.

■ ACKNOWLEDGMENTS

M.S.F. is supported by an ARC Laureate Fellowship. J.T.H. is supported by US NSF award DMR-11-05224. Preparation of Bi_2Se_3 was supported by NSF (DMR-0952716). Photoemission measurements were performed at the Soft X-ray Beamline of the Australian Synchrotron. Identification of commercial materials or equipment does not imply recommendation or endorsement by the National Institute of Standards and Technology, nor does it imply that the materials or equipment identified are necessarily the best available for the purpose.

■ REFERENCES

(1) Hasan, M. Z.; Kane, C. L. Colloquium: Topological Insulators. *Rev. Mod. Phys.* **2010**, *82*, 3045−3067.

(2) Zhang, H. J.; Liu, C.-X.; Qi, X.-L.; Fang, Z.; Zhang, S.-C. Topological Insulators in Bi_2Se_3, Bi_2Te_3 and Sb_2Te_3 with a Single Dirac Cone on the Surface. *Nat. Phys.* **2009**, *5*, 438−442.

(3) Fu, L.; Kane, C. L.; Mele, E. J. Topological Insulators in Three Dimensions. *Phys. Rev. Lett.* **2007**, *98*, 106803−106806.

(4) R. Takahasi, R.; S. Murakami, S. Gapless Interface States between Topological Insulators with Opposite Dirac Velocities. *Phys. Rev. Lett.* **2011**, *107*, 166805−166808.

(5) Gibson, Q. D.; Schoop, L. M.; Weber, A. P.; Ji, H.; Nadi-Perge, S.; Drozdov, I. K.; Beidenkopf, H.; Sadowski, J. T.; Fedorov, A.; Yazdani, A.; et al. Termination-Dependent Topological Surface States of the Natural Superlattice Phase Bi_4Se_3. *Phys. Rev. B* **2013**, *88*, 081108−081112(R).

(6) Valla, T.; Ji, H.; Schoop, L. M.; Weber, A. P.; Pan, Z.-H.; Sadowski, J. T.; Vescovo, E.; Fedorov, A. V.; Caruso, A. N.; Gibson, Q. D.; et al. Topological Semimetal in a Bi-Bi_2Se_3 Infinitely Adaptive Superlattice Phase. *Phys. Rev. B* **2012**, *86*, 241101−241105(R).

(7) Hewitt, A. S.; Wang, J.; Boltersdorf, J.; Maggard, P. A.; Dougherty, D. B. Coexisting Bi and Se Surface Terminations of Cleaved Bi_2Se_3 Single Crystals. *J. Vac. Sci. Technol., B* **2014**, *32*, 04E103−04E108.

(8) Atuchin, V. V.; Golyashov, V. A.; Kokh, K. A.; Korolkov, I. V.; Kozhukhov, A. S.; Kruchinin, V. N.; Makarenko, S. V.; Pokrovsky, L. D.; Prosvirin, I. P.; Romanyuk, K. N.; et al. Formation of Inert Bi_2Se_3(0001) Cleaved Surface. *Cryst. Growth Des.* **2011**, *11*, 5507−5514.

(9) He, X.; Zhou, W.; Wang, Z. Y.; Zhang, Y. N.; Shi, J.; Qu, R. Q.; Yarmoff, J. A. Surface Termination of Cleaved Bi_2Se_3 Investigated by Low Energy Ion Scattering. *Phys. Rev. Lett.* **2013**, *110*, 156101−156105.

(10) Reis, D. D.; Barreto, L.; Bianchi, M.; Ribeiro, G. A. S.; Soares, E. A.; Silva, W. S.; Carvalho, V. E.; Rawle, J.; Hoesch, M.; Nicklin, C.; et al. Surface Structure of Bi_2Se_3(111) Determined by Low-Energy Electron Diffraction and Surface X-ray Diffraction. *Phys. Rev. B* **2013**, *88*, 041404−041407(R).

(11) Kong, D.; Cha, J. J.; Lai, K.; Peng, H.; Analytis, J. G.; Meister, S.; Chen, Y.; Zhang, H.-J.; Fisher, I. R.; Shen, Z.-X.; et al. Rapid Surface Oxidation as a Source of Surface Degradation Factor for Bi_2Se_3. *ACS Nano* **2011**, *5*, 4698−4703.

(12) Yashina, L. V.; Sanchez-Barriga, J.; Scholz, M. R.; Volykhov, A. A.; Sirotina, A. P.; Neudachina, V. S.; Tamm, M. E.; Varykhalov, A.; Marchenko, D.; Springholz, G.; et al. Negligible Surface Reactivity of Topological Insulators Bi_2Se_3 and Bi_2Te_3 towards Oxygen and Water. *ACS Nano* **2013**, *7*, 5181−5191.

(13) Golyashov, V. A.; Kokh, K. A.; Makarenko, S. V.; Romanyuk, K. N.; Prosvirin, I. P.; Kalinkin, A. V.; Tereshchenko, O. E.; Kozhukhov, A. S.; Sheglov, D. V.; Eremeev, S. V.; et al. Inertness and Degradation of (0001) Surface of Bi_2Se_3 Topological Insulator. *J. Appl. Phys.* **2012**, *112*, 113702−113706.

(14) Butch, N. P.; Kirshenbaum, K.; Syers, P.; Sushkov, A. B.; Jenkins, G. S.; Drew, H. D.; Paglione, J. Strong Surface Scattering in Ultrahigh-Mobility Bi_2Se_3 Topological Insulator Crystals. *Phys. Rev. B* **2010**, *81*, 241301−241304(R).

(15) Kuroda, K.; Ye, M.; Schwier, E. F.; Nurmamat, M.; Shirai, K.; Nakatake, M.; Ueda, S.; Miyamoto, K.; Okuda, T.; Namatame, H.; et al. Experimental Verification of the Surface Termination in the Topological Insulator $TlBiSe_2$ using Core-Level Photoelectron Spectroscopy and Scanning Tunneling Microscopy. *Phys. Rev. B* **2013**, *88*, 245308−245314.

(16) Edmonds, M. T.; Hellerstedt, J.; Tadich, A.; Schenk, A.; O'Donnell, K. M.; Tosado, J.; Butch, N. P.; Syers, P.; Paglione, J.; Fuhrer, M. S. Air-Stable Electron Depletion of Bi_2Se_3 Using Molybdenum Trioxide into the Topological Regime. *ACS Nano* **2014**, *8*, 6400−6406.

(17) http://srdata.nist.gov/xps/.

(18) Benia, H. M.; Lin, C.; Kern, K.; Ast, C. R. Reactive Chemical Doping of the Bi_2Se_3 Topological Insulator. *Phys. Rev. Lett.* **2011**, *107*, 177602−177606.

(19) Bianchi, M.; Guan, D.; Bao, S.; Mi, J.; Iversen, B. B.; King, P. D. C.; Hofmann, P. Coexistence of the Topological State and a Two-Dimensional Electron Gas on the Surface of Bi_2Se_3. *Nat. Commun.* **2010**, *1*, 128−132.

(20) Muntwiler, M.; Zhu, X.-Y. Image-Potential States on the Metallic (111) Surface of Bismuth. *New J. Phys.* **2008**, *10*, 113018−113029.

(21) Zangwill, A. *Physics at Surfaces*; Cambridge University Press: New York, 1988.

(22) Waitkins, G. R.; Shutt, R.; Kinney, I. W.; McReynolds, J. P. *Inorganic Syntheses*; Wiley Publishing: New York, 1946; Vol. 2.

(23) Gann, R. D.; Wen, J.; Xu, Z.; Gu, G. D.; Yarmoff, J. A. Surface Restructuring in Sputter-Damaged $Bi_2Sr_2CaCu_2O_{8+\delta}$. *Phys. Rev. B* **2011**, *84*, 165411−165416.
(24) Sakamoto, K.; Matsuhata, H.; Kyoya, K. I.; Miki, K.; Sakamoto, T. Abrupt Si/Ge/Si(001) Interfaces Fabricated with Bi as a Surfactant. *Jpn. J. Appl. Phys.* **1994**, *33*, 2307−2310.
(25) Jun, S. W.; Fetzer, C. M.; Lee, R. T.; Shurtleff, J. K.; Stringfellow, G. B. Bi Surfactant Effects on Ordering in GaInP Grown by Organometallic Vapor-Phase Epitaxy. *Appl. Phys. Lett.* **2000**, *76*, 2716−2718.
(26) Hirahara, T.; Bihlmayer, G.; Sakamoto, Y.; Yamada, M.; Miyazaki, H.; Kimura, S.; Blügel, S.; Hasegawa, S. Interfacing 2D and 3D Topological Insulators: Bi(111) Bilayer on Bi_2Te_3. *Phys. Rev. Lett.* **2011**, *107*, 166801−166805.
(27) Murakami, S. Quantum Spin Hall Effect and Enhanced Magnetic Response by Spin-Orbit Coupling. *Phys. Rev. Lett.* **2006**, *97*, 236805−236808.